MOLECULAR AND CELLULAR BIOLOGY, Mar. 2010, p. 1528–1540 Vol. 30, No. 6
0270-7306/10/$12.00 doi:10.1128/MCB.01018-09

Distribution of Activator of G-Protein Signaling 3 within the Aggresomal Pathway: Role of Specific Residues in the Tetratricopeptide Repeat Domain and Differential Regulation by the AGS3 Binding Partners Giα and Mammalian Inscuteable[▽]

Ali Vural,[1] Sadik Oner,[1] Ningfei An,[1] Violaine Simon,[1]‡ Dzwokai Ma,[2] Joe B. Blumer,[1] and Stephen M. Lanier[1]*

Department of Cell and Molecular Pharmacology and Experimental Therapeutics, Medical University of South Carolina, Charleston, South Carolina 29425,[1] and Department of Molecular, Cellular and Developmental Biology, University of California, Santa Barbara, Santa Barbara, California 93106[2]

Received 1 August 2009/Returned for modification 10 September 2009/Accepted 30 December 2009

AGS3, a receptor-independent activator of G-protein signaling, is involved in unexpected functional diversity for G-protein signaling systems. AGS3 has seven tetratricopeptide (TPR) motifs upstream of four G-protein regulatory (GPR) motifs that serve as docking sites for Giα-GDP. The positioning of AGS3 within the cell and the intramolecular dynamics between different domains of the proteins are likely key determinants of their ability to influence G-protein signaling. We report that AGS3 enters into the aggresome pathway and that distribution of the protein is regulated by the AGS3 binding partners Giα and mammalian Inscuteable (mInsc). Giα rescues AGS3 from the aggresome, whereas mInsc augments the aggresome-like distribution of AGS3. The distribution of AGS3 to the aggresome is dependent upon the TPR domain, and it is accelerated by disruption of the TPR organizational structure or introduction of a nonsynonymous single-nucleotide polymorphism. These data present AGS3, G-proteins, and mInsc as candidate proteins involved in regulating cellular stress associated with protein-processing pathologies.

The discovery of AGS3 (GPSM1) and related accessory proteins revealed unexpected functional diversity for G-protein signaling systems (8, 36). AGS3 is involved in a number of different cellular activities, including asymmetric cell division during neuronal development (30), neuronal plasticity and addiction (9, 10, 12, 38, 39), autophagy (27), membrane protein trafficking (17), cardiovascular function (7), and metabolism (7). AGS3 is a multidomain protein consisting of seven tetratricopeptide repeats (TPR) in the amino-terminal portion of the protein and four G-protein regulatory (GPR) motifs in the carboxyl region of the protein. Each of the GPR motifs binds and stabilizes the GDP-bound conformation of Gα (Giα, Gtα, and Gi/oα), essentially behaving as a guanine nucleotide dissociation inhibitor. As such, AGS3 may be complexed with up to four Gα and function as an alternative binding partner for Gα independently of the classical heterotrimeric Gαβγ. Despite the clearly demonstrated function of AGS3 and the related protein LGN (GPSM2 or AGS5) in various model organisms and a fairly solid, basic biochemical understanding of the interaction of a GPR motif with Gα, the signals that operate "upstream" and/or "downstream" of AGS3 or an AGS3-Gi/oα complex are not well defined.

AGS3 and other GPR proteins may regulate G-protein signaling directly by influencing the interaction of Gα with Gβγ or another Gα binding partner. In addition, a portion of Gα in the cell is complexed with GPR proteins to various degrees, and this interaction is regulated. Ric-8A interacts with an AGS3-Giα complex in a manner somewhat analogous to the interaction of a G-protein-coupled receptor with heterotrimeric Gαβγ, promoting nucleotide exchange and the apparent dissociation of AGS3 and Giα-GDP (37). The specific impact of AGS3 and other GPR proteins on signaling events is likely dependent upon where the individual protein is positioned within the cell and the nature of intra- and intermolecular interactions that influence the interaction of the GPR motif with Gi/oα.

The TPR domain of AGS3 is an important determinant of its positioning within the cell through its interaction with specific binding partners (1, 8, 28, 36). As part of a broader effort to address the fundamental questions of AGS3 "positioning" and control of G-protein interaction, we focused upon the roles of individual TPR domains. Endogenous and ectopically expressed wild-type AGS3 is nonhomogeneously distributed in the cytoplasm, with obvious punctate structures, and it may be present at the cell periphery. Disruption of the TPR organizational structure by targeted amino acid substitutions or introduction of a nonsynonymous single-nucleotide polymorphism redistributes AGS3 to punctate structures throughout the cytoplasm that are similar in appearance to the preaggresomal assemblies or aggregates observed in neurodegenerative diseases. Upon cellular stress, both wild-type and TPR-modified AGS3 migrate, in a microtubule-dependent manner, to a perinuclear aggresome. The distribution of AGS3 to the aggresome is dependent upon the TPR domain, and it is differentially regulated by Giα and mammalian Inscuteable (mInsc),

* Corresponding author. Mailing address: Colcock Hall, Medical University of South Carolina, Charleston, SC 29425. Phone: (843) 792-7134. Fax: (843) 792-5110. E-mail: lanier@musc.edu.

‡ Present address: Univ. Paris Diderot-Paris 7, Unité de Biologie Fonctionnelle et Adaptative (BFA), CNRS-EAC 7059, Physiologie de l'Axe Gonadotrope, 75013 Paris, France.

▽ Published ahead of print on 11 January 2010.

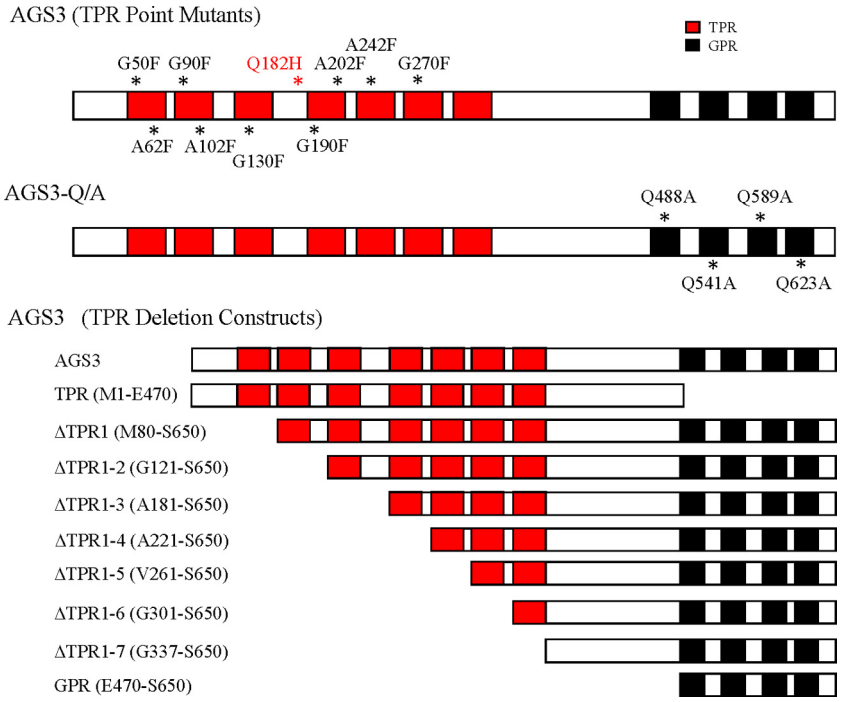

FIG. 1. Schematic representation of the different point mutations and truncation constructs. The amino acid numbers refer to rat AGS3. In the top illustration of AGS3, the asterisks indicate sites of individual mutations, and the red asterisk (Q182H) indicates the nonsynonymous single-nucleotide polymorphism corresponding to rs28507185 in human AGS3 that results in the amino acid substitution Q185H. Each generated construct contained only one of the illustrated mutations. In the middle illustration of AGS3-Q/A, a single construct contained all four Q/A mutations rendering the protein incapable of binding Gα.

which bind to the GPR and TPR domains, respectively, of AGS3. These data present AGS3 and G-proteins as candidate proteins involved in regulating cellular stress associated with protein-processing pathologies and suggest that this involvement can be manipulated to therapeutic advantage.

MATERIALS AND METHODS

Materials. $Gi\alpha_3$ antisera was a kind gift from Thomas W. Gettys (Pennington Biomedical Research Institute). Catalase antisera was a kind gift from Inderjit Singh (Medical University of South Carolina). COS-7 (CRL-1651), human embryonic kidney cells (HEK-293) (CRL-1573), and Chinese hamster ovary (CHO) cells were purchased from American Type Culture Collection (Manassas, VA). Cath.a-differentiated (CAD) cells were provided by James Bear (University of North Carolina, Chapel Hill, NC). Human Giα3 cDNA (wild-type and mutant cDNA encoding the amino acid change Q204L) was obtained from the Missouri Science and Technology cDNA Resource Center. QuikChange XL site-directed mutagenesis kits were purchased from Stratagene (La Jolla, CA). Bicinchoninic acid (BCA) protein assay kits were obtained from Thermo Scientific (Roford, IL). MG 132, β-tubulin antibody, nocodazole, poly-D-lysine hydrobromide, Igepal CA-630, trans-epoxysuccinyl-L-leucylamido-(4-guanidino)butane (E 64), pepstatin A, and Geneticin (G418) were purchased from Sigma (St. Louis, MO). Affinity-purified anti-peptide AGS3 antibodies were generated as previously described (2, 28). Antisera were also generated in the laboratory of D. Ma by immunization of rabbits with a glutathione *S*-transferase (GST)–AGS3 fusion protein encoded by the GPR domain (A461 to S650) of AGS3 (16a). Antibodies to calnexin (ab2798), EEA-1 (ab15846), COX IV (ab16056), LAMP-2 (ab25631), clathrin (ab2731), and vimentin (ab8978) were purchased from Abcam Inc. (Cambridge, MA) and used in accordance with the manufacturer's instructions. GM130 antibody (clone 35/GM130) was obtained from BD Biosciences (San Jose, CA). Lipofectamine 2000, anti-mouse and anti-rabbit antibodies conjugated to Alexa Fluor 594, transferrin antibody (clone H68.4), cell culture media, hypoxanthine aminopterin and thymidine, and fetal bovine serum were purchased from Invitrogen (Carlsbad, CA). GammaBind G Sepharose was purchased from GE Healthcare Bio-Sciences (Princeton, NJ). All other reagents were obtained as previously described (1, 28, 31).

Generation of TPR-modified AGS3 constructs. The TPR domain of AGS3 was modified by progressive deletion of TPR motifs or site-directed mutagenesis of conserved residues within individual TPR motifs. (Fig. 1). Deletion mutants were generated by PCR with primers designed to facilitate subcloning into pcDNA3 and pEGFP-N1. The 5′ primers also contained a Kozak consensus sequence for translational initiation. The PCRs were generally performed using 100 μM primers and 20 ng of template DNA in a total volume of 50 μl (annealing at 94°C, with 30 cycles of 1.5 min at 94°C, 1 min at 60°C, and 2 min at 72°C and a final extension of 1 × 10 min at 72°C). All plasmids were sequenced to confirm the fidelity of the cDNA amplification.

Primers used to generate specific constructs were as follows: reverse primer pEGFP-N1, 5′-GGATCCCGGCTGGCACCTGGCGGACATTG-3′; reverse primer pcDNA3, 5′-GAATTCTTAGCTGGCACCTGGCGGACATTG-3′; and forward primers ΔTPR1-AGS3(M80-S650), 5′-CCCCTCGAGACCATGGGGGAAGCCAAGGCCAGT-3′; ΔTPR1-2-AGS3(G121-S650), 5′-CCCCTCGAGACCATGGGGGAAGCGAGAGCACTCTACAAC-3′; ΔTPR1-3-AGS3(A181-S650), 5′-CCCCTCGAGACCATGGCCCAGGGCAGAGCCTATGGCAAC-3′; ΔTPR1-4-AGS3(A221-S650), 5′-CCCCTCGAGACCATGGCTGAGAGGAGAGCCTACAGCAAC-3′; ΔTPR1-5-AGS3(V261-S650), 5′-CCCCTCGAGACCATGGTGGAAGCACAGGCTTGCTACAGT-3′; ΔTPR1-6-AGS3(G301-S650), 5′-CCCCTCGAGACCATGGGAGAGGGCCGAGCTTGCTGGAGC-3′; ΔTPR1-7-AGS3(G337-S650), 5′-CCCCTCGAGACCATGGGAGACCGAAATGGAGAGCTCACG-3′; and ΔTPR/linker-AGS3(E470-S650), 5′-CCCCTCGAGACCATGGAGGAGTGTTTCTTCGATCTGCTG-3′.

Cell culture, transfection, and fractionation. CAD cells, HEK-293 cells, CHO cells, and NG108-15 cells were grown, respectively, in Dulbecco's modified Eagle's medium (DMEM) with 10% fetal bovine serum (FBS), DMEM/F12 with 10% FBS, DMEM (high glucose) with 5% FBS, Ham's F12 with 10% FBS, and DMEM (high glucose) with 10% FBS supplemented with hypoxanthine aminopterin and thymidine. All media were supplemented with penicillin (100 units/ml), streptomycin (100 μg/ml), and amphotericin B (Fungizone; 0.25 μg/ml). Cells at 70 to 80% confluence in 60- or 100-mm tissue culture dishes were transiently transfected with cDNA constructs (0.25 to 5 μg) using Lipofectamine 2000.

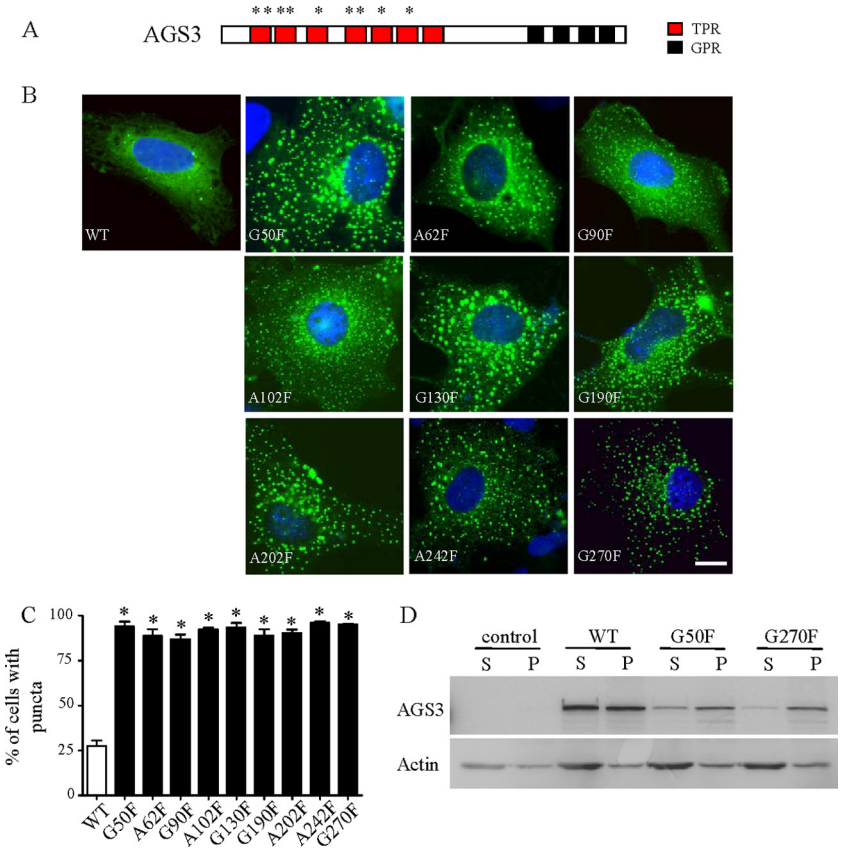

FIG. 2. Effect of single-amino-acid substitutions on the subcellular distribution of AGS3. (A) Schematic illustration of AGS3 domain organization. The TPR domain of AGS3 was modified by site-directed mutagenesis (asterisks) of conserved residues as described in Materials and Methods. (B) COS-7 cells were transfected with pEGFP-N1::AGS3 constructs and processed for fluorescence microscopy as described in Materials and Methods. Images are shown at a magnification of ×63; the bar represents 10 μm. (C) Quantitative analysis of cells exhibiting punctate structures containing AGS3 following expression of AGS3-WT and AGS3 mutants. Data are presented as means ± standard errors of the means (SEMs) ($n = 3$). *, $P < 0.05$ compared to results for AGS3-WT. (D) Subcellular distribution of TPR-modified AGS3 (50 μg of protein/lane). pEGFP-N1::AGS3-transfected cells were lysed in hypotonic lysis buffer and processed for immunoblotting as described in Materials and Methods. S, supernatant resulting from centrifugation at 100,000 × *g*; P, pellet resulting from centrifugation at 100,000 × *g*. Data in panels B and D are representative of 3 to 10 experiments.

Transfection efficiency was 30 to 40%. HEK-293 cells were stably transfected at 60 to 70% confluence (2 μg of human pEGFPN1::AGS3-Q185H) in a 100-mm dish and then split into two 100-mm dishes. Transfected cells were selected by growth in DMEM containing 1 mg/ml G418.

For separation of a crude cytosol and membrane fraction, cells were harvested after 48 h and resuspended in hypotonic buffer (5 mM Tris-HCl [pH 7.4], 5 mM EDTA, 5 mM EGTA, 0.2 μg/ml protease inhibitor) with a 26-gauge syringe. The samples were centrifuged at 100,000 × *g* for 30 min at 4°C to generate a crude membrane pellet and the resulting supernatant containing cytosol. The membrane pellets were washed once with 4 volumes of membrane buffer (50 mM Tris-HCl [pH 7.4], 5 mM $MgCl_2$, 0.6 mM EDTA). In some experiments, harvested cells were lysed with buffer containing 1% Igepal CA-630 to generate

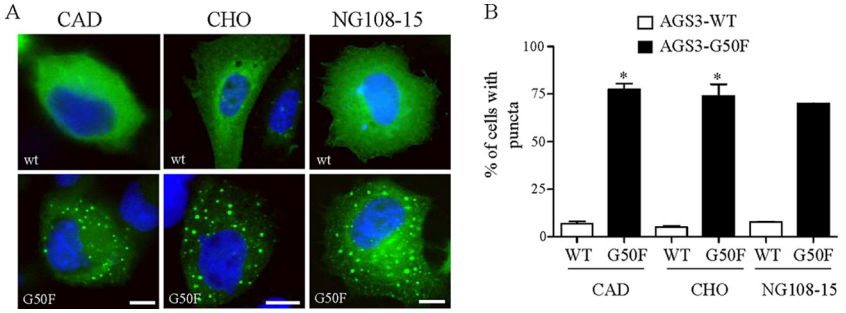

FIG. 3. Subcellular distribution of wild-type AGS3 (AGS3-WT) and AGS3-G50F in different cell types. (A) CAD, CHO, and NG108-15 cell lines were transfected with AGS3-WT and AGS3-G50F in pEGFP-N1 and processed for fluorescence microscopy. The images presented are representative of one (NG108-15) or three (CHO and CAD) separate experiments. Bars, 10 μm. (B) Quantitative analysis of cells exhibiting punctate structures containing AGS3 following expression of AGS3-WT and the AGS3 mutant. Data are presented as means ± SEMs ($n = 3$). *, $P < 0.05$ compared to results for AGS3-WT for each cell type.

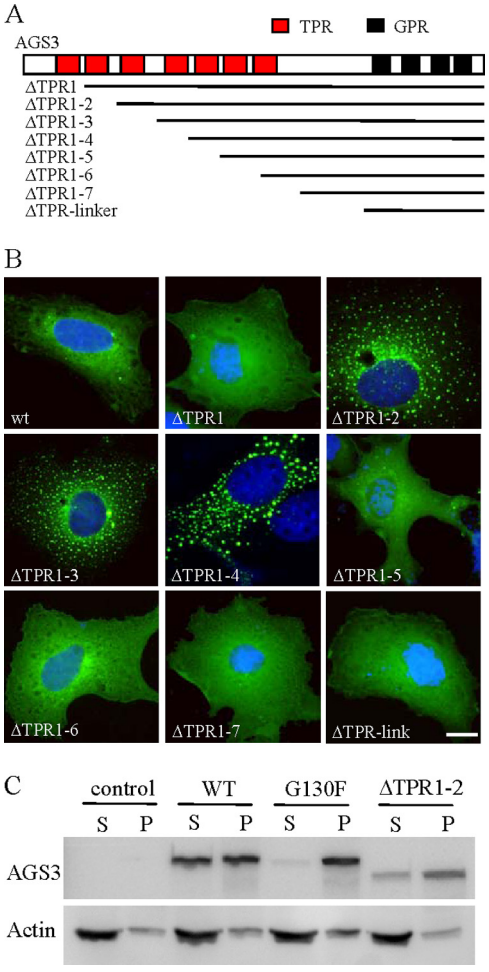

FIG. 4. Effect of amino-terminal deletions on the subcellular distribution of AGS3. (A) Schematic representation of TPR-modified AGS3 constructs. The TPR domain of AGS3 was modified by deletion mutagenesis as described in Materials and Methods. (B) Fluorescent images of COS-7 cells expressing wild-type (wt) and TPR-modified AGS3-enhanced GFP. Images are representative of 70 to 80% of the cells examined for any given construct in at least three separate transfections. Bar, 10 μm. (C) Subcellular distribution of TPR-modified AGS3 (50 μg of protein/lane). COS-7 cells transfected with the pEGFP-N1::AGS3 constructs were lysed in hypotonic lysis buffer and processed for immunoblotting as described in Materials and Methods. S, supernatant resulting from centrifugation at 100,000 × *g*; P, pellet resulting from centrifugation at 100,000 × *g*. The images shown are representative of three experiments.

whole-cell lysates as previously described (1). Samples were solubilized in Laemmli sample buffer and processed for SDS-PAGE and immunoblotting.

Cell imaging. Cells on poly-D-lysine-coated glass coverslips were washed twice with cell-washing solution (CWS; 137 mM $NaCl_2$, 2.6 mM KCl, 1.8 mM KH_2PO_4, and 10 mM Na_2HPO_4) at 4°C and then fixed with 4% paraformaldehyde–4% sucrose in CWS for 15 min. The cells were then washed three times with CWS and permeabilized by incubation with 0.2% Triton X-100 in CWS (5 min). Cells were then incubated sequentially with 4% normal donkey serum (1 h), primary antibody (1 h), and a secondary antibody, goat anti-rabbit or anti-mouse antibody–Alexa Fluor 594 (1 μg/ml), with intervening washes with CWS. Slides were then mounted with glass coverslips and visualized using a Leica DM5500B fluorescence microscope with a Hamamatsu ORCA ER digital camera and SimplePCI software (Compix Inc.). Images were obtained from approximately the middle plane of the cells and saved as TIF files. Differential interference contrast images were obtained, using a Leica TCS SP2 AOBS laser-scanning confocal microscope. Unless indicated otherwise, images in the figures are shown at a magnification of ×63. Nucleic acids were stained by the addition of 4′,6-diamidino-2-phenylindole ([DAPI] 1 μg/ml) to the diluted secondary antibody. Antibodies were used at dilutions recommended by the manufacturer, and antibody dilution mixtures were centrifuged at 10,000 × *g* for 10 min prior to use. For detection of endogenous AGS3, we used affinity-purified antibody generated against the GPR domain of AGS3 at a final concentration of ~0.008 μg/μl.

The percentage of cells exhibiting peripheral punctate structures (>20) and/or perinuclear aggresomes together with a general reduction in diffuse cytoplasmic distribution was determined by visual examination of 200 cells from at least three separate experiments. Data were analyzed by Student's *t* test or analysis of variance, with significant differences between groups determined by Tukey's *a posteriori* test, using GraphPad Prism version 4.03 for Windows (GraphPad Software, San Diego, CA).

RESULTS

TPR domains and AGS3 localization. An individual TPR consists of a pair of antiparallel α-helices (~34 amino acids) arranged in a highly conserved tertiary structure. The overall amino acid sequence of TPR domains is highly degenerate, but the domains retain a conserved tertiary structure and are characterized by conserved residues at positions 8 and 20 (24, 25). To address the role of individual TPR motifs in determining AGS3 subcellular location, we first introduced single-amino-acid changes within a single TPR motif of AGS3 targeting the signature residues for a TPR motif (Fig. 1) and expressed the proteins in COS-7 cells. The TPR-modified AGS3 constructs exhibited striking changes in their subcellular distribution patterns compared to those of the wild-type AGS3 and appeared as a constellation of intracellular punctate structures in over 80% of any given transfected cell population (Fig. 2). The punctate constellation of the TPR-modified AGS3 proteins

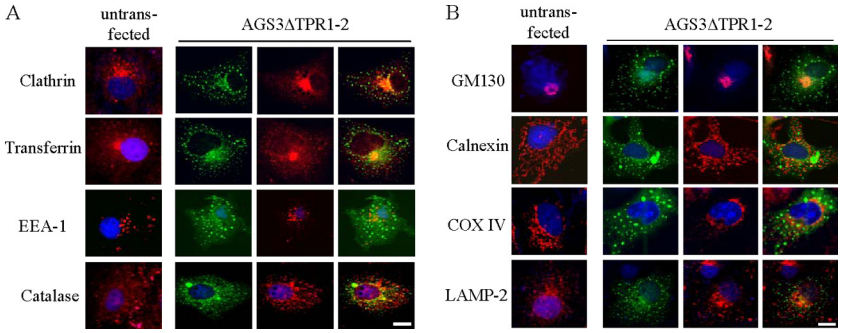

FIG. 5. Comparison of the subcellular distribution of TPR-modified AGS3 and vesicle and organelle markers. COS-7 cells were transfected with pEGFP-N1::AGS3ΔTPR1-2 and processed for immunofluorescence microscopy. The data presented (magnification, ×63) are representative of two to five experiments, and the images are representative of >80% of the transfected cells in each set of experiments. For AGS3ΔTPR1-2 images, left panels represent AGS3ΔTPR1-2, middle panels represent the organelle marker, and right panels are the merged image. Bars, 10 μm.

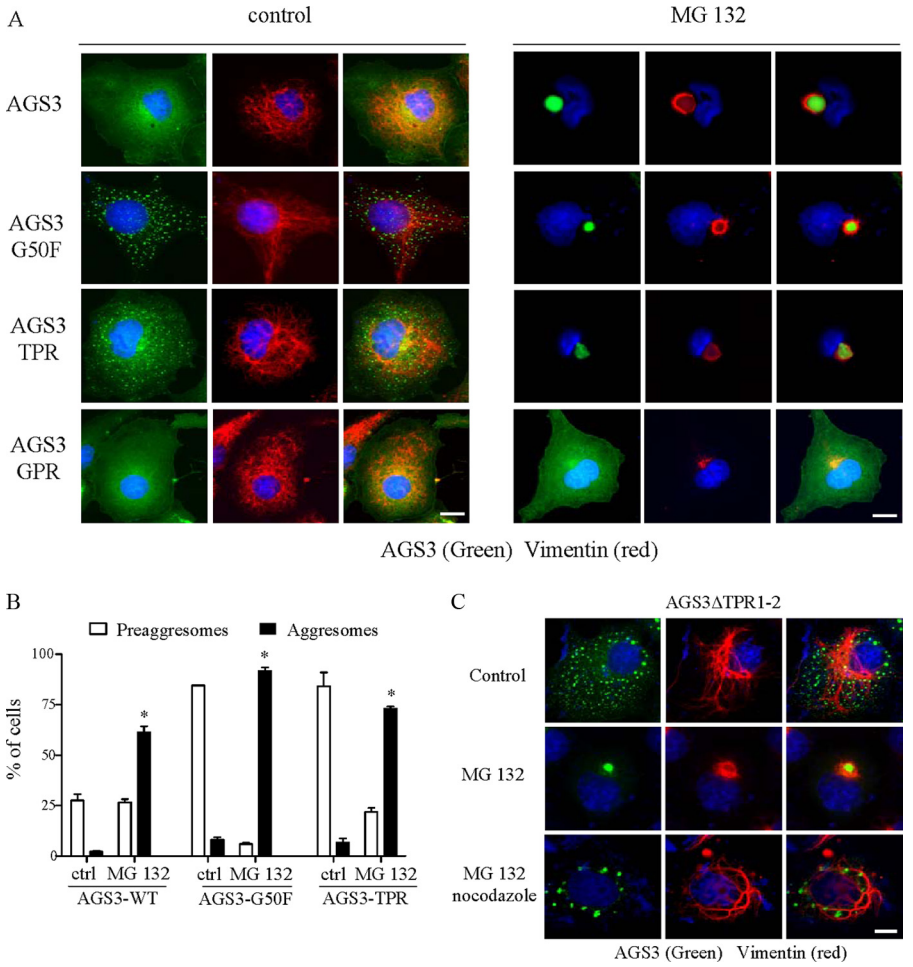

FIG. 6. Influence of the proteasome inhibitor MG 132 on the subcellular distribution of AGS3. (A) COS-7 cells were transfected with wild-type or TPR-modified AGS3 (AGS3-TPR [M1 to E470] or AGS3-GPR [E470 to S650]) in pEGFP-N1. Thirty-six hours after transfection, cells were incubated with MG 132 (10 μM) for 12 h, and then the cells were processed for immunofluorescence microscopy. The images presented are representative of 2 to 10 separate transfections. (B) Two hundred cells from each series of experiments shown in panel A were examined, and the percentage of cells exhibiting peripheral preaggresome puncta or perinuclear aggresomes containing AGS3 was determined. Data are expressed as means ± SEMs ($n = 3$). *, $P < 0.05$ compared to the value obtained for control cells not treated with MG 132. (C) COS-7 cells were transfected with pEGFP-N1::AGS3ΔTPR1-2 and incubated with MG 132 (10 μM) or MG 132 (10 μM) plus nocodazole (2.3 μM) for 12 h. The images shown are representative of three to five separate transfections. The right panel in each image set is the merged image. Bar, 10 μm.

was also observed in CHO cells and in the neuronal cell lines CAD and NG108-15 (Fig. 3). The immunofluorescence distribution of wild-type AGS3 was a mixed pattern that oscillated between a diffuse cytoplasmic staining, cortical staining, and the punctate structure, which is similar to that observed for endogenous AGS3 in PC12 cells and primary cultures of rat hippocampal neurons (5).

Thus, substitution of a single, signature amino acid in any of the seven TPR motifs resulted in the same redistribution of AGS3. However, progressive truncation of the amino-terminal end suggests that individual TPR motifs play specific roles in this redistribution, as AGS3ΔTPR1-2 (AGS3 G121 to S650), AGS3ΔTPR1-3 (AGS3 A181 to S650), and AGS3ΔTPR1-4 (AGS3 A221 to S650) exhibited the punctate constellation appearance, whereas AGS3ΔTPR1 (M80 to S650), AGS3ΔTPR1-5 (V261 to S650), AGS3ΔTPR1-6 (G301 to S650), and AGS3ΔTPR1-7 (G337 to S650) did not (Fig. 4). These data also suggest a higher-order structure for the TPR domain, as observed for other proteins with multiple TPR motifs (4). Wild-type and TPR-modified AGS3 proteins were expressed at similar levels (Fig. 2D and 4C), indicating that the distribution of the TPR-modified AGS3 to the punctate structures was not simply due to higher levels of expression. Subcellular fractionation indicated that compared to that of wild-type AGS3, the appearance of the puncta with the TPR-modified AGS3 was associated with redistribution of the protein to a membrane pellet following cell lysis with nondetergent hypotonic buffer (Fig. 2D and 4C).

We then asked whether these punctate structures were associated with defined intracellular organelles and whether the subcellular distribution of the TPR-modified protein was regulated. The distribution pattern of the TPR-modified AGS3 proteins resembles that of subcellular vesicles; however, it was distinct from early endosomes and the cycling vesicles defined by transferrin and clathrin (Fig. 5A). The TPR-modified AGS3 constructs also did not localize to the *cis*-Golgi apparatus

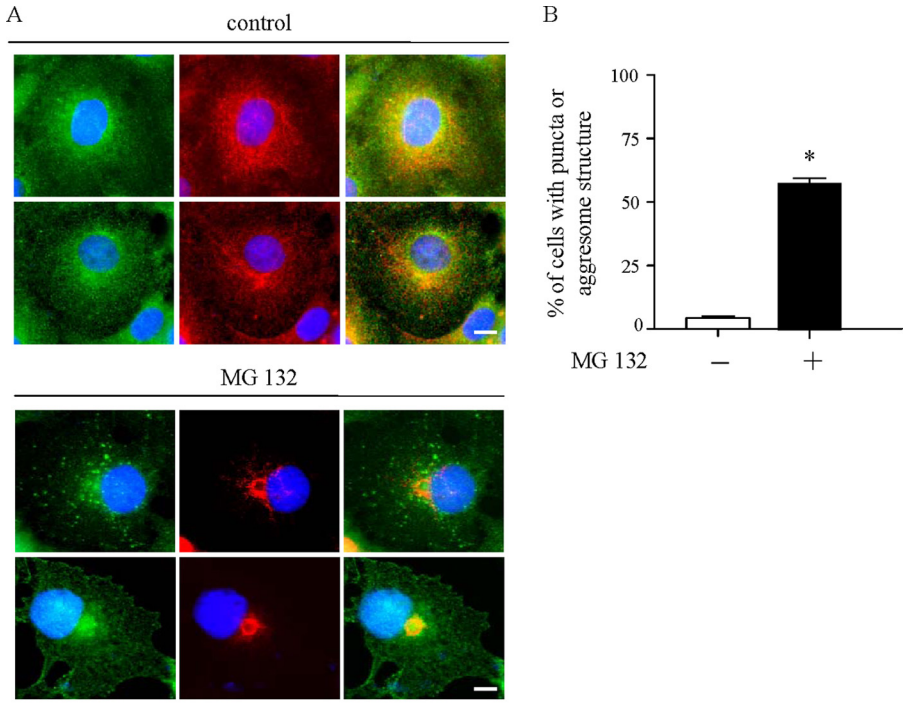

FIG. 7. Influence of proteasome inhibitors on subcellular distribution of endogenous AGS3. (A) COS-7 cells were treated with vehicle or MG 132 as described in the legend to Fig. 6 and processed for immunofluorescence microscopy as described in Materials and Methods. Both the upper panel (control) and the lower panel (MG 132) present two individual cell images for illustration purposes. (B) Quantitative analysis of cells exhibiting punctate structures containing AGS3. Data are expressed as means ± SEMs ($n = 4$). −, without MG 132; +, with MG 132; $P < 0.05$ compared to the control without MG 132 treatment. The right panel in each image set is the merged image.

(GM130), endoplasmic reticulum (calnexin), mitochondria (COX IV), peroxisomes (catalase), or lysosomes (LAMP-2) (Fig. 5B).

AGS3 and the aggresomal pathway. The punctate constellation observed with the TPR-modified AGS3 protein is remarkably similar to inclusion bodies, protein clusters, or aggresome-like induced structures observed in neurodegenerative diseases or upon cellular stress, hormonal challenge, and ectopic expression of certain proteins (14, 18, 22, 26). Upon cellular stress, such entities often assemble as mature aggresomes at the microtubule organizing center, where they are surrounded by the intermediate filament protein vimentin and further processed by autophagy. The aggresome pathway is implicated in inducible nitric oxide synthase (iNOS) signaling, neurodegenerative diseases, aberrant cell growth, cystic fibrosis, general protein processing, and the biology of asymmetric cell division (11, 13, 18, 19, 21, 26, 33, 34). Two features of the aggresome pathway are its sensitivity to cellular stress, such as nutrient deprivation or proteasome inhibition, and the role of microtubules in aggresome assembly.

To determine if the punctate structures observed for AGS3 were preaggresomal entities, we asked if cellular stress influenced the subcellular distribution of wild-type and TPR-modified AGS3. Treatment of cells expressing wild-type AGS3 or TPR-modified AGS3 with the proteasome inhibitor MG 132 resulted in a dramatic redistribution of the peripheral puncta to a perinuclear aggresome (Fig. 6A and B). In some cells, the movement of wild-type and TPR-modified AGS3 to the aggresome is also observed to various degrees without proteasome inhibition, likely reflecting an accumulation of the protein in the aggresome over time. This process is likely accelerated and augmented by proteasome inhibition. The core assembly of the TPR-modified AGS3 protein in the aggresome was embedded within a vimentin "cage," and the redistribution of the TPR-modified AGS3 proteins into this aggresome structure was blocked by the disruption of microtubules with nocodazole (Fig. 6C). Thus, the peripheral constellation represents preaggresomal structures that move to the perinuclear aggresome in a microtubule-dependent manner.

The preaggresomal distribution of AGS3 and its subsequent movement to the perinuclear aggresome requires the TPR domain of AGS3 as it is observed with AGS3-TPR (AGS3 M1 to E470) but not with AGS3-GPR (AGS3 E470 to S650) (Fig. 6A). We next determined the effect of proteasome inhibition on the distribution of endogenous AGS3 in the aggresome pathway by immunofluorescence microscopy of COS-7 cells. Cell treatment with the proteasome inhibitor MG 132 resulted in the appearance of defined puncta or preaggresomal structures containing endogenous AGS3 in the cytoplasm as well as accumulated AGS3 protein in the perinuclear aggresome embedded in a "vimentin cage," similar to, although perhaps less robust than, the images obtained with transfected, green fluorescent protein (GFP)-tagged protein (Fig. 7).

Distribution of AGS3 containing a nonsynonymous single-nucleotide polymorphism. Given the dramatic changes in the trafficking of AGS3 introduced by single-residue point muta-

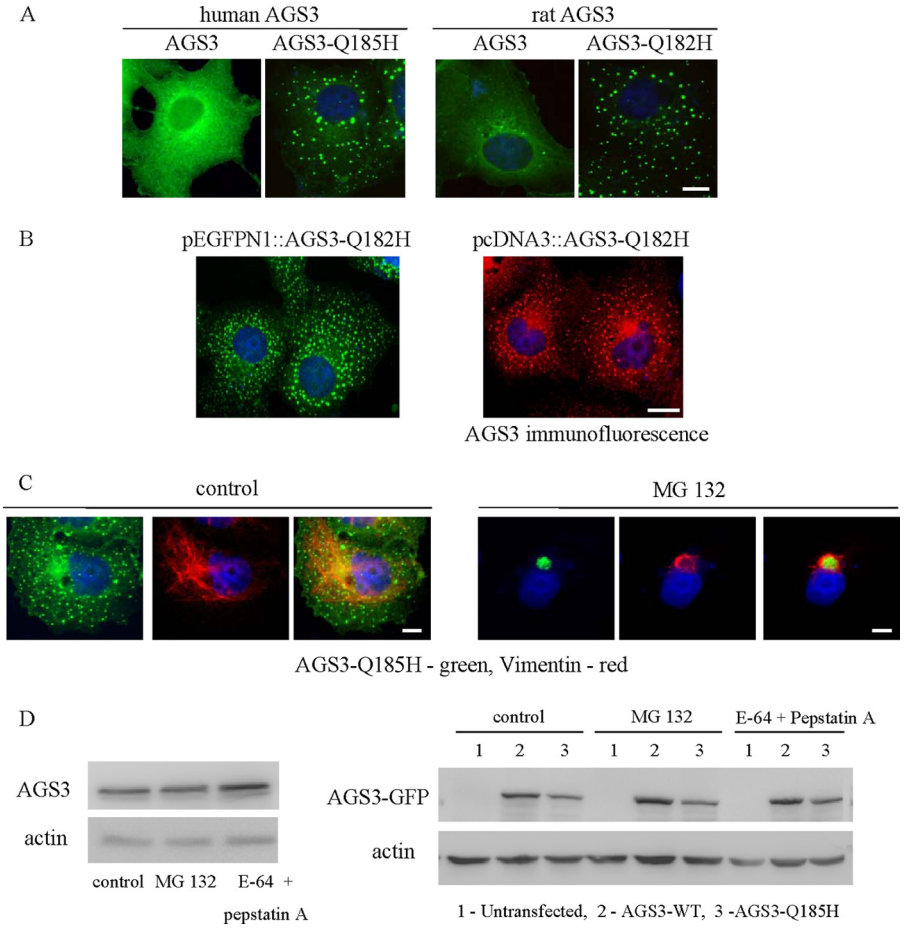

FIG. 8. Subcellular distribution of human and rat AGS3 containing a nonsynonymous single-nucleotide polymorphism. (A) COS-7 cells were transfected with pEGFP-N1::AGS3 or pEGFP-N1::AGS3-SNP (human Q185H or rat Q182H) and processed for fluorescence microscopy. (B) COS-7 cells were transfected with pEGFP-N1::AGS3-Q182H (left panel) or pcDNA3::AGS3-Q182H (right panel), with the latter transfectants processed for immunofluorescence microscopy with PEP32 AGS3 antibody. Quantitative analyses of AGS3-Q185H-transfected cells exhibiting peripheral preaggresome puncta containing AGS3-Q185H are illustrated in Fig. 10B. Similar percentages were observed for AGS3-Q182H-transfected cells. (C) COS-7 cells were transfected with pEGFP-N1::AGS3-Q185H and treated with MG 132 as described in the legend to Fig. 6. The images shown are representative of 5 to 10 (A and C) or 2 (B) separate series of experiments. The right panel in each image set is the merged image of the left and middle panels. Bar, 10 μm. (D) Influence of proteasome inhibitors and lysosome inhibitors on expression of endogenous and transfected AGS3. Untransfected COS-7 cells (left panel) or COS-7 cells transfected with pEGFP-N1::AGS3 or pEGFP-N1::AGS3-Q185H (0.25 μg) (right panel) were incubated with MG 132 (10 μM for 12 h) or E-64 (28 μM) and pepstatin A (14 μM) for 24 h. Cells were lysed in lysis buffer (5 mM Tris-HCl [pH 7.4], 150 mM $NaCl_2$, 5 mM EDTA, 5 mM EGTA, 0.2 μg/ml protease inhibitor, 1% Igepal CA-630). Endogenous AGS3 in the left panel was detected with affinity-purified antibody generated against a GST-AGS3 fusion protein encoding the GPR domain (A461 to S650) of AGS3, whereas transfected AGS3-GFP in the right panel was detected with PEP 32 AGS3 antibody (28). The immunoblots (100 mg of protein/lane) are representative of three independent experiments.

tions in the TPR domain and the potential connections with human disease, we searched various databases for any single-nucleotide polymorphisms (SNPs) within the TPR domains. The NCBI SNP database (dbSNP) revealed a nonsynonymous SNP (Q185H) just adjacent to the fourth TPR domain in human AGS3. (The database lists four SNPs in the coding region of GPSM1 [http://www.ncbi.nlm.nih.gov/SNP/snp_ref.cgi?locusId=26086]. Two of the SNPs are synonymous [exon 13], and two result in a change in codon usage [rs28507185 and rs60980157]. rs28507185 is found within the TPR domain at amino acid 185, whereas rs60980157 is found in the linker region of AGS3 at amino acid 368. We focused on the nonsynonymous SNP in the TPR domain.) Introduction of this SNP into human AGS3 or an analogous location in rat AGS3 (Q182H) resulted in a subcellular distribution that exactly mirrored that observed with the individual TPR-modified constructs described earlier (Fig. 2 and 8), indicating potential functional pathology for individuals with this allelic variant. The differences in the subcellular distribution of wild-type and AGS3-SNP were observed with both GFP-tagged and untagged protein (Fig. 8B), and MG 132 treatment redistributed AGS3-SNP to the perinuclear aggresome (Fig. 8C). Immunoblots of cell extracts indicated that neither proteasome inhibition nor lysosome inhibition increased the level of endogenous AGS3 or expressed wild-type AGS3 and AGS3-Q185H, suggesting that the protein does not primarily turn over through the proteasome or lysosome pathway (Fig. 8D).

The fluorescent preaggresomal structures were clearly associated with a subset of vesicle-like structures, as revealed by differential interference contrast images (Fig. 9). The various

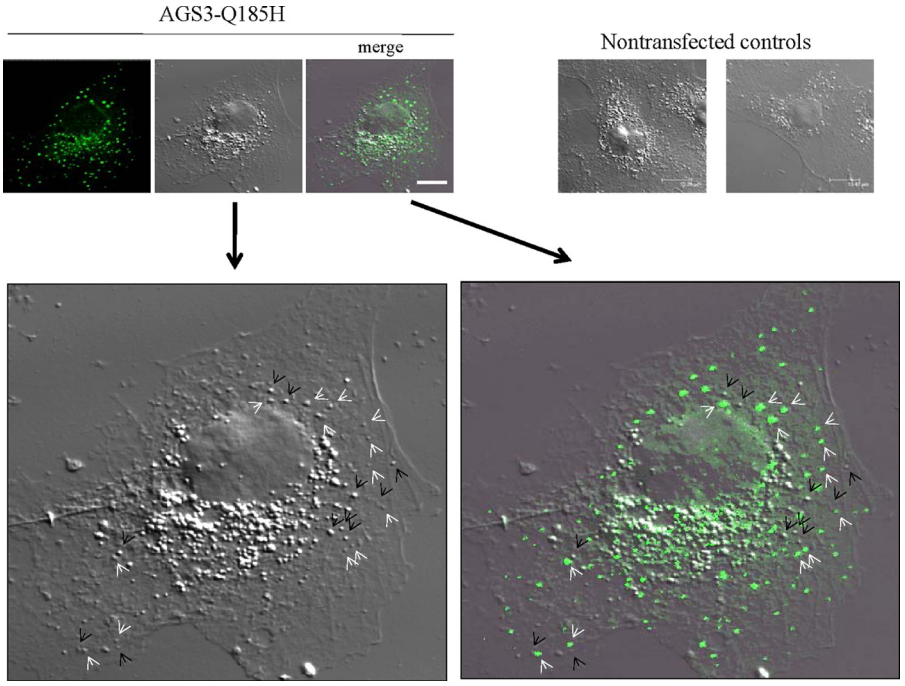

FIG. 9. Differential interference contrast images of COS-7 cells expressing AGS3-Q185H. The top three panels on the left indicate the fluorescent image, the differential interference contrast image, and the merged image from cells transfected with pEGFP-N1::AGS3-Q185H. Bar, 10 μm. The two upper right panels provide two separate differential interference contrast images from control untransfected cells to provide comparisons for any expression-induced changes in images. The two images in the lower panel are enlargements of the upper left panels as indicated by the arrows. Rounded vesicle-like structures free of fluorescence signals are indicated with black arrow points, and those colocalizing with the fluorescent eGFP tag are indicated with white arrow points. Data illustrated are representative of two to five separate experiments.

vesicle-like structures visualized by differential interference contrast microscopy have different refractive indexes consistent with different content and/or positioning within the cell. However, it was not possible to define a specific phenotype of vesicle-like structures associated with the fluorescence signal. Expression of AGS3-Q185H did not alter the number or type of vesicle-like structures (Fig. 9, top left panels versus top right panels).

Influence of AGS3 binding partners on AGS3 localization in the aggresome pathway. The subcellular distribution of AGS3, LGN, and/or their *Drosophila melanogaster* ortholog Pins is regulated by various binding partners, including Giα, inscuteable, and/or Frmpd1. The latter two proteins interact with AGS3 through its TPR domain. AGS3 contains four GPR motifs in its carboxyl terminus region, and coexpression of Giα or Goα can alter the subcellular distribution of AGS3, increasing its presence at the cell cortex to various degrees. The interaction of AGS3 with Frmpd1 stabilizes a membrane-associated population of AGS3, and the interaction of AGS3 with Frmpd1 and Giα3 is apparently mutually exclusive (1). Interaction of inscuteable with LGN and/or the *D. melanogaster* ortholog Pins positions the AGS3-like proteins in a specific region of the cell cortex during asymmetric cell division, where they interact with Giα while also binding to inscuteable (20, 32, 42). Thus, we asked if the aggresomal distribution of AGS3 is regulated by its binding partners.

Coexpression of Giα1, Giα2, Giα3, or Goα eliminated the punctate constellation observed with the human AGS3-Q185H SNP or the analogous rat AGS3-Q182H SNP (Fig. 10 and 11). The rescue of AGS3-SNP was not observed with cotransfection of a constitutively active mutant of Giα3 (Q204L), consistent with the observed specificity of the GPR motifs for the GDP-bound form of Giα proteins (Fig. 10A). Introduction of the same nonsynonymous SNP into AGS3-Q/A, which cannot bind G-protein due to substitution of alanine for a conserved Q in each of the GPR motifs, resulted in a similar redistribution of the protein to the punctate structures; however, the redistribution of AGS3-Q/A containing the nonsynonymous SNP was not rescued by coexpression of Giα3, indicating the direct requirement for G-protein binding to the GPR motifs for the rescue of AGS3-SNP (Fig. 11A).

Giα may prevent the accumulation of AGS3-Q185H in the aggresomal pathway by sequestering the protein to a membrane compartment. It is not clear whether coexpression of G-protein actually rescues AGS3 from the punctate structures after it has already trafficked to the structure or whether Giα3 binding prevents AGS3 from entering into or exiting from the aggresome pathway. As a first step to address this issue, we generated HEK-293 cells stably expressing AGS3-Q185H and determined the effect of transient expression of Giα3 on its subcellular distribution. The punctate distribution observed for AGS3-Q185H in the transient expression system was also apparent in HEK-293 cells stably expressing AGS3-Q185H, and this was also rescued by expression of Giα3 (Fig. 11B). These data suggest that Giα can interact with AGS3 in the puncta and induce a conformational change in the protein that moves AGS3 out of the preaggresomal structures. However, this conclusion depends somewhat upon the half-life of AGS3 in the preaggresomal structures. If there is rapid turnover of AGS3 in the puncta (i.e., less

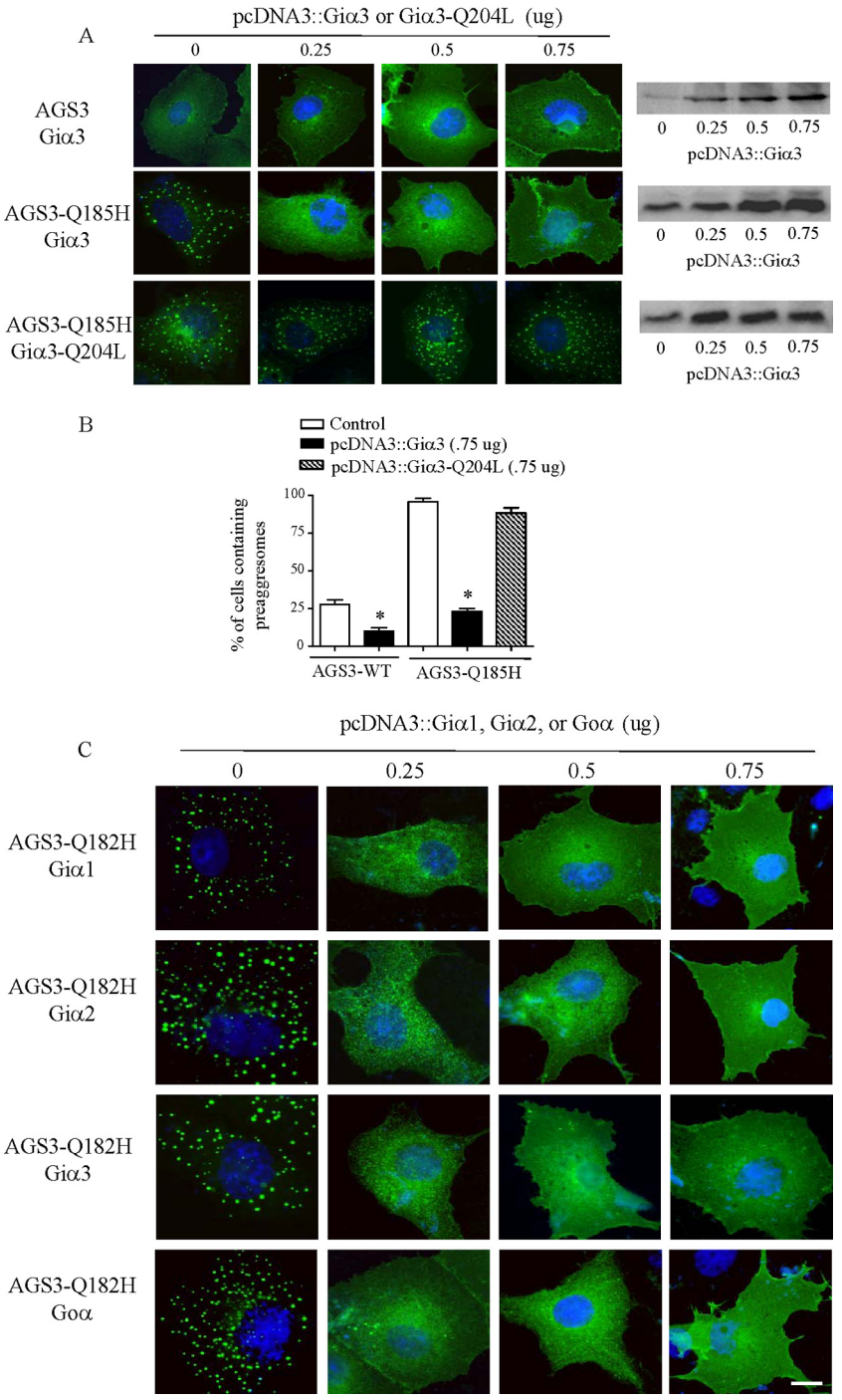

FIG. 10. Influence of Gα coexpression on the subcellular distribution of human AGS3 and AGS3-Q185H. (A) COS-7 cells were transfected with pEGFP-N1::AGS3 or pEGFP-N1::AGS3-Q185H (0.5 μg) with or without increasing amounts of pcDNA3::Giα3 or constitutively active Giα3-Q204L and were processed for fluorescence microscopy. Data are representative of three to five separate experiments. Top immunoblot, 30 μg of protein/lane; middle and bottom immunoblots, 50 μg of protein/lane. (B) Quantitative analysis of cells exhibiting peripheral preaggresome puncta containing AGS3. Data are expressed as means ± SEMs ($n = 3$). *, $P < 0.05$ versus results for the control. (C) COS-7 cells were transfected with pEGFP-N1::AGS3-Q182H (0.5 μg) (rat cDNA) with and without increasing amounts of pcDNA3::Giα1, pcDNA3::Giα2, pcDNA3::Giα3, or pcDNA3::Goα. Images presented for each set of experiments are representative of 70 to 80% of the transfected cells.

than 12 h), then the elimination of the puncta upon expression of Giα could result from preventing newly translated AGS3 from entering into the preaggresomal structures. Giα coexpression also markedly reduced the distribution of wild-type AGS3 and AGS3-Q185H to the perinuclear aggresome following proteasome inhibition (Fig. 12).

Interestingly, the AGS3 binding partner mInsc actually resulted in an opposite response to that observed with Giα3 with

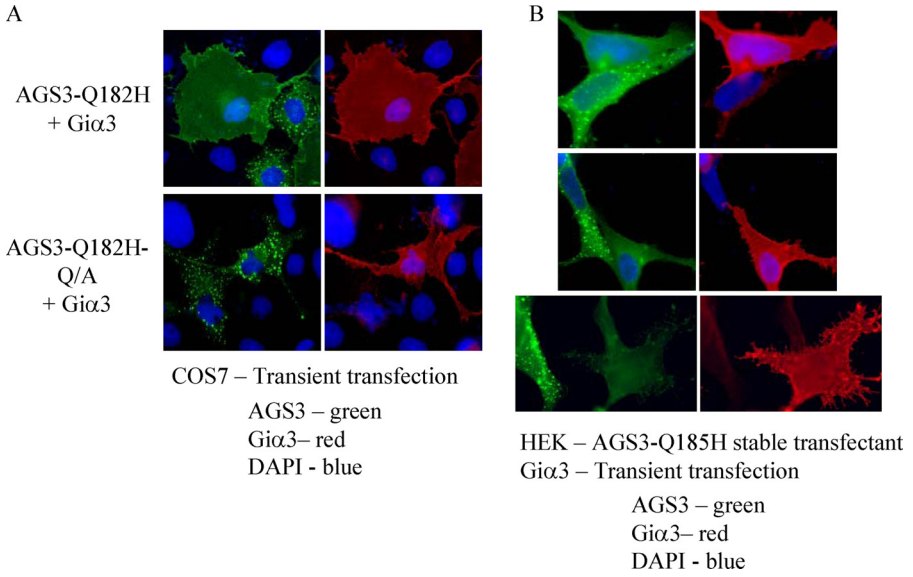

FIG. 11. Influence of Giα3 on subcellular distribution of AGS3-SNP and AGS3-SNP-Q/A. (A) AGS3-Q182H and AGS3-Q182H-Q/A in pEGFP-N1 (0.5 μg) were expressed in COS-7 cells with pcDNA3::Giα3 (1 μg) and processed for fluorescence microscopy as described in Materials and Methods. Data are representative of three to five separate experiments. (B) HEK-293 cells in 6-well dishes stably expressing AGS3-Q185H were transiently transfected with pcDNA3::Giα3 (1 μg/well). Each set of panels presents different fields of cells. Data are representative of three experiments.

respect to the subcellular distribution of AGS3 (Fig. 13). inscuteable binds to the TPR domain of AGS3 and LGN as well as the *D. melanogaster* ortholog Pins, and this interaction is important for asymmetric cell division. Coexpression of mInsc resulted in a redistribution of wild-type AGS3 to preaggresomal puncta and the perinuclear region, mimicking the effect of either TPR modification or proteasome inhibition on wild-type AGS3 subcellular distribution (Fig. 13). These data suggest that mInsc, which interacts with the TPR domain of AGS3, induces a conformational change in the protein that mimics that induced by the introduction of single-residue mutations in TPR domains. Indeed, the mInsc-induced presence of AGS3 in the perinuclear region was also reversed by the expression of Giα3 (Fig. 13).

DISCUSSION

The subcellular distributions of AGS3 and the related protein LGN, which possess a similar domain structure and exhibit 65% amino acid identity, are intimately related to their functionality, but we do not fully understand what regulates the positioning of the proteins within the cell. Certainly, the distribution of the proteins is dynamic and regulated to various degrees by interaction with binding partners such as inscuteable, G-proteins, Frmpd1, and/or NuMA (1, 8). LGN may localize in the nucleus during interphase, depending upon the cell type, with various degrees of distribution at the cell cortex, but moves in a regulated manner to the spindle pole during cell division and is also found at the midbody during cytokinesis (5, 6). AGS3 is generally found in the cytoplasm, exhibiting a nonhomogeneous appearance with various degrees of distribution at the cell cortex, and it also localizes to the spindle pole during cell division (5; R. Nadella, J. B. Blumer, G. Jia, M. Kwon, F. Qian, F. Sedic, T. Wakatsuki, W. E. Sweeney, P. D. Wilson, S. M. Lanier, and F. Park, submitted for publication). Both the TPR and the GPR domains of the two proteins play a role in the positioning of the proteins.

Endogenous AGS3 may appear in the cell as small, nonhomogeneous punctate structures that are poorly defined and variable in appearance (5; Nadella et al., submitted). A similar distribution is observed for AGS3 upon transfection-mediated expression in various cell types (1, 2, 17, 28). Expression of simply the TPR domain of AGS3 reveals a more prominent nonhomogeneous punctate appearance, whereas expression of the GPR domain reveals a more general, diffuse distribution within the cytosol (28), suggesting that the two domains play dynamic roles in regulating the subcellular distribution of the full-length protein. As a first approach to address this issue, we focused upon the TPR domain of AGS3 as a determinant of such movement. Our goal was to define the role of specific regions within the TPR domain that regulate the subcellular positioning of AGS3 and influence its interaction with G-proteins.

The observed range of subcellular distribution of AGS3 likely reflects regulated movement of the protein among different subcellular compartments in ways that we do not fully understand. Interaction of endogenous AGS3 with Gαi may serve as a point of regulation for the distribution of AGS3 in the aggresome pathway. The aggresomal distribution of both wild-type AGS3 and TPR-modified AGS3 suggests that the punctate constellation observed upon disruption of the ordered TPR array reflects a site along the normal trafficking pathway where AGS3 is retained or directed as a result of the protein conformation stabilized by the TPR modification. It is not fully understood how AGS3 and G-proteins may function mechanistically within these various functional modules. However, with respect to the aggresome pathway, Gβγ interacts with class II histone deacetylases 4 and 5 (35) and regulates the cytoplasmic motor protein dynein (29). The movement of proteins within the aggresome pathway is actually regulated by the

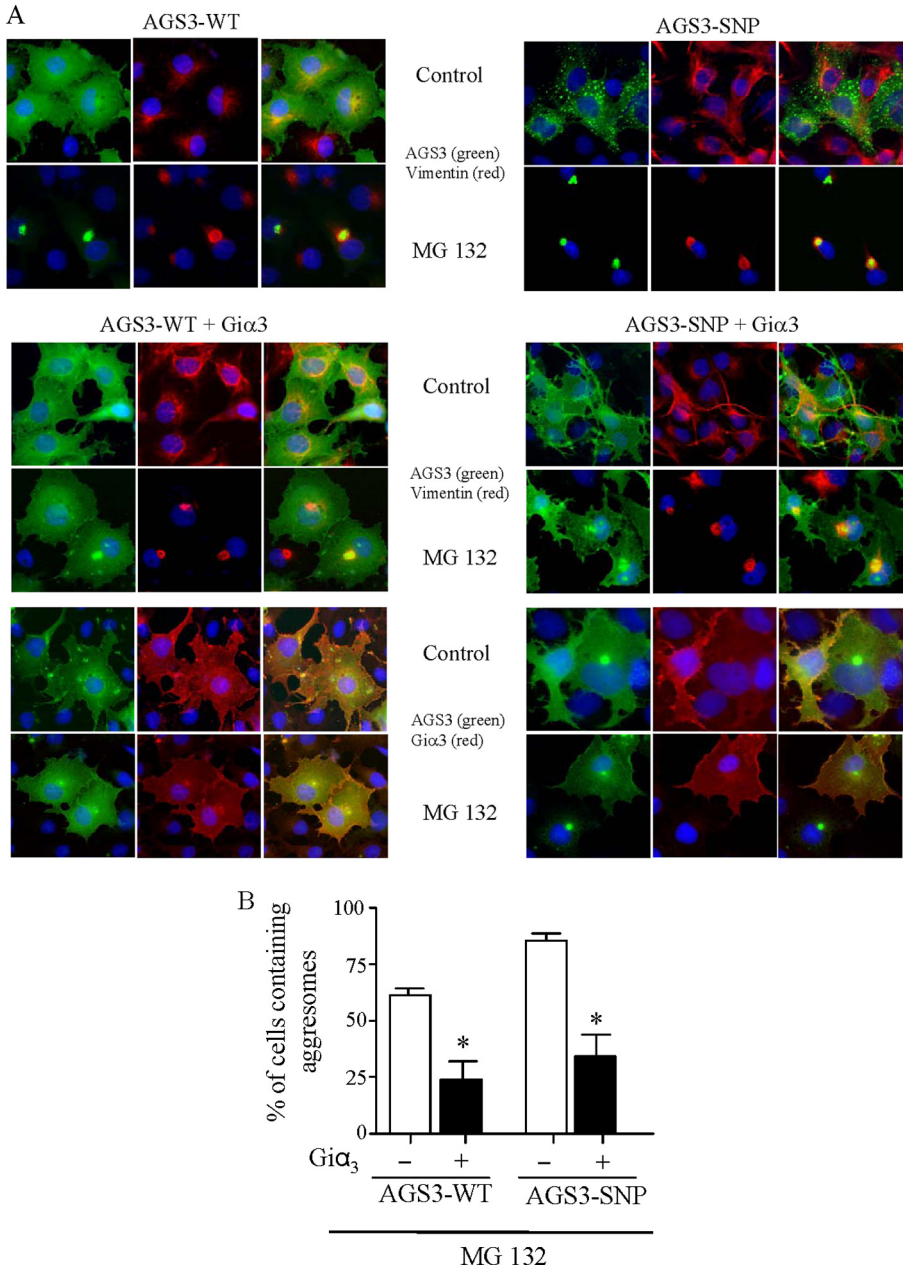

FIG. 12. Influence of Giα3 on subcellular distribution of AGS3 following proteasome inhibition. (A) COS-7 cells were transfected with pEGFP-N1::AGS3 or pEGFP-N1::AGS3-Q185H (0.25 μg) with and without pcDNA3::Giα3 (0.5 μg) and processed for fluorescence microscopy. The right panel in each image set is the merged image of the left and middle panels. (B) Quantitative analysis of cells exhibiting aggresomes containing AGS3. Data are presented as means ± SEMs ($n = 3$). *, $P < 0.05$ versus results obtained in the absence of $Gi\alpha_3$.

class II histone deacetylase 6 and dynein-dynactin complexes (19, 23). Overall, these observations strongly suggest that AGS3 and G-proteins provide functional connectivity among these diverse cell functions in ways that we do not yet fully appreciate.

The presence of AGS3 in the aggresomal pathway and the regulation of this distribution by G-proteins and mInsc are of particular interest, given the roles of aggresomes, AGS3, G-proteins, and inscuteable in asymmetric cell division, autophagy, and/or vesicle formation (3, 8, 15, 16, 27, 34, 40, 41). AGS3 expression is enriched in the central nervous system, where such aggresomal structures, protein clusters, and/or inclusion bodies are key features of neurodegenerative diseases associated with cellular stress. Cellular stress and associated pathologies involving altered microenvironment or aging may push a cell over a threshold in terms of certain functions, such as handling various conformationally fragile or aggregation-prone proteins, be they the wild type or allelic variants. The ability of AGS3 binding partners to regulate distribution of AGS3 to the aggresomal pathway suggests a regulatory mechanism that could be manipulated to therapeutic advantage.

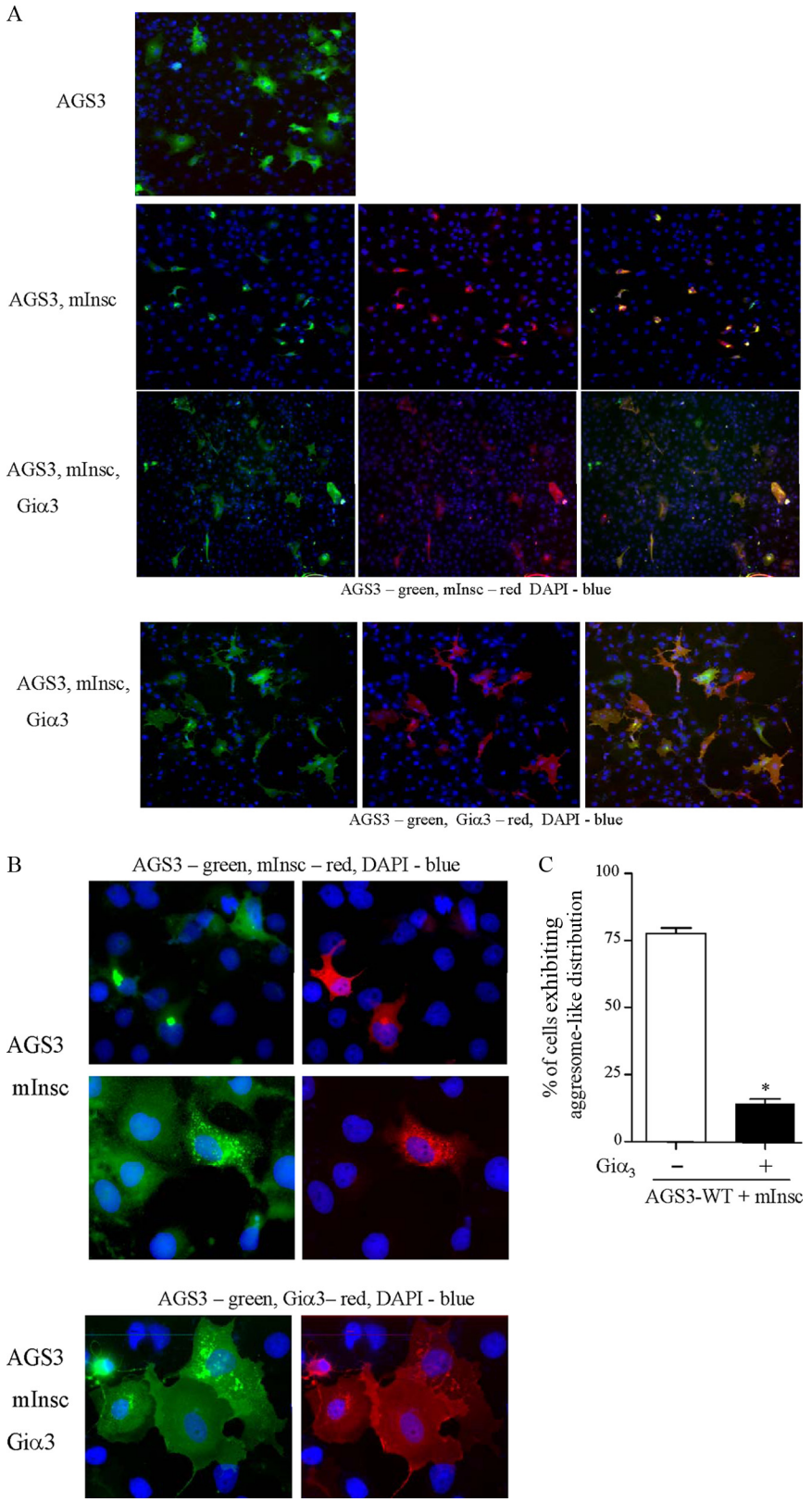

FIG. 13. Influence of mInsc on the subcellular distribution of AGS3. (A and B) COS-7 cells were transfected with pEGFP-N1::AGS3 without and with pcDNA3::mInsc (0.5 μg) or with pcDNA3::mInsc (0.5 μg) and pcDNA3::Giα3 (1 μg) and processed for fluorescence microscopy and immunoblotting. The images (magnification, ×10 for panel A and ×63 for panel B) presented are representative of two to four separate transfections. The right panel in each three-image set presents the merge image of the left and middle panels. (C) Quantitative analysis of cells exhibiting perinuclear aggresomes containing AGS3. Data are expressed as means ± SEMs ($n = 3$). *, $P < 0.05$ versus results obtained in the absence of $Gi\alpha_3$.

ACKNOWLEDGMENTS

This work was supported by grants from the National Institutes of Health (NS24821 and DA025896 to S.M.L.).

We thank Maureen Fallon, Heather Bainbridge, and Sandra Klatt for technical assistance. We appreciate the input of Paul McDermott (Medical University of South Carolina) related to aggresome fractionation. We thank Nathalie Pizzinat (Institut National de la Santé et de la Recherche Médicale U388) for generating the AGS3-eGFP construct, Jim W. Zheng (Medical University of South Carolina) for discussions regarding single-nucleotide polymorphism databases, Inderjit Singh (Medical University of South Carolina) for catalase antibody, Thomas W. Gettys (Pennington Biomedical Research Center) for Giα3 antisera, James Bear (University of North Carolina) for CAD cells, and Jurgen Knoblich (Molecular Biology Institute) for mInsc cDNA and antibody.

REFERENCES

1. **An, N., J. B. Blumer, M. L. Bernard, and S. M. Lanier.** 2008. The PDZ and band 4.1 containing protein Frmpd1 regulates the subcellular location of activator of G-protein signaling 3 and its interaction with G-proteins. J. Biol. Chem. **283:**24718–24728.
2. **Bernard, M. L., Y. K. Peterson, P. Chung, J. Jourdan, and S. M. Lanier.** 2001. Selective interaction of AGS3 with G-proteins and the influence of AGS3 on the activation state of G-proteins. J. Biol. Chem. **276:**1585–1593.
3. **Blackmer, T., E. C. Larsen, C. Bartleson, J. A. Kowalchyk, E. J. Yoon, A. M. Preininger, S. Alford, H. E. Hamm, and T. F. Martin.** 2005. G protein betagamma directly regulates SNARE protein fusion machinery for secretory granule exocytosis. Nat. Neurosci. **8:**421–425.
4. **Blatch, G. L., and M. Lassle.** 1999. The tetratricopeptide repeat: a structural motif mediating protein-protein interactions. Bioessays **21:**932–939.
5. **Blumer, J. B., L. J. Chandler, and S. M. Lanier.** 2002. Expression analysis and subcellular distribution of the two G-protein regulators AGS3 and LGN indicate distinct functionality. Localization of LGN to the midbody during cytokinesis. J. Biol. Chem. **277:**15897–15903.
6. **Blumer, J. B., R. Kuriyama, T. W. Gettys, and S. M. Lanier.** 2006. The G-protein regulatory (GPR) motif-containing Leu-Gly-Asn-enriched protein (LGN) and Gialpha3 influence cortical positioning of the mitotic spindle poles at metaphase in symmetrically dividing mammalian cells. Eur. J. Cell Biol. **85:**1233–1240.
7. **Blumer, J. B., K. Lord, T. L. Saunders, A. Pacchioni, C. Black, E. Lazartigues, K. J. Varner, T. W. Gettys, and S. M. Lanier.** 2008. Activator of G protein signaling 3 null mice. I. Unexpected alterations in metabolic and cardiovascular function. Endocrinology **149:**3842–3849.
8. **Blumer, J. B., A. V. Smrcka, and S. M. Lanier.** 2007. Mechanistic pathways and biological roles for receptor-independent activators of G-protein signaling. Pharmacol. Ther. **113:**488–506.
9. **Bowers, M. S., F. W. Hopf, J. K. Chou, A. M. Guillory, S. J. Chang, P. H. Janak, A. Bonci, and I. Diamond.** 2008. Nucleus accumbens AGS3 expression drives ethanol seeking through G betagamma. Proc. Natl. Acad. Sci. U. S. A. **105:**12533–12538.
10. **Bowers, M. S., K. McFarland, R. W. Lake, Y. K. Peterson, C. C. Lapish, M. L. Gregory, S. M. Lanier, and P. W. Kalivas.** 2004. Activator of G protein signaling 3: a gatekeeper of cocaine sensitization and drug seeking. Neuron **42:**269–281.
11. **Burnett, B. G., and R. N. Pittman.** 2005. The polyglutamine neurodegenerative protein ataxin 3 regulates aggresome formation. Proc. Natl. Acad. Sci. U. S. A. **102:**4330–4335.
12. **Fan, P., Z. Jiang, I. Diamond, and L. Yao.** 2009. Up-regulation of AGS3 during morphine withdrawal promotes cAMP superactivation via adenylyl cyclase 5 and 7 in rat nucleus accumbens/striatal neurons. Mol. Pharmacol. **76:**526–533.
13. **Fortun, J., W. A. Dunn, Jr., S. Joy, J. Li, and L. Notterpek.** 2003. Emerging role for autophagy in the removal of aggresomes in Schwann cells. J. Neurosci. **23:**10672–10680.
14. **Garcia-Mata, R., Y. S. Gao, and E. Sztul.** 2002. Hassles with taking out the garbage: aggravating aggresomes. Traffic **3:**388–396.
15. **Gauthier-Fisher, A., D. C. Lin, M. Greeve, D. R. Kaplan, R. Rottapel, and F. D. Miller.** 2009. Lfc and Tctex-1 regulate the genesis of neurons from cortical precursor cells. Nat. Neurosci. **12:**735–744.
16. **Gohla, A., K. Klement, R. P. Piekorz, K. Pexa, S. vom Dahl, K. Spicher, V. Dreval, D. Haussinger, L. Birnbaumer, and B. Nurnberg.** 2007. An obligatory requirement for the heterotrimeric G protein Gi3 in the antiautophagic action of insulin in the liver. Proc. Natl. Acad. Sci. U. S. A. **104:**3003–3008.

16a. **Groves, B., H. Abrahamsen, H. Glingan, M. Frantz, L. Mavor, J. Bailay, and D. Ma.** PLoS ONE, in press.

17. **Groves, B., Q. Gong, Z. Xu, C. Huntsman, C. Nguyen, D. Li, and D. Ma.** 2007. A specific role of AGS3 in the surface expression of plasma membrane proteins. Proc. Natl. Acad. Sci. U. S. A. **104:**18103–18108.
18. **Johnston, J. A., C. L. Ward, and R. R. Kopito.** 1998. Aggresomes: a cellular response to misfolded proteins. J. Cell Biol. **143:**1883–1898.
19. **Kawaguchi, Y., J. J. Kovacs, A. McLaurin, J. M. Vance, A. Ito, and T. P. Yao.** 2003. The deacetylase HDAC6 regulates aggresome formation and cell viability in response to misfolded protein stress. Cell **115:**727–738.
20. **Knoblich, J. A., L. Y. Jan, and Y. N. Jan.** 1999. Deletion analysis of the Drosophila Inscuteable protein reveals domains for cortical localization and asymmetric localization. Curr. Biol. **9:**155–158.
21. **Kolodziejska, K. E., A. R. Burns, R. H. Moore, D. L. Stenoien, and N. T. Eissa.** 2005. Regulation of inducible nitric oxide synthase by aggresome formation. Proc. Natl. Acad. Sci. U. S. A. **102:**4854–4859.
22. **Kopito, R. R.** 2000. Aggresomes, inclusion bodies and protein aggregation. Trends Cell Biol. **10:**524–530.
23. **Kopito, R. R.** 2003. The missing linker: an unexpected role for a histone deacetylase. Mol. Cell **12:**1349–1351.
24. **Magliery, T. J., and L. Regan.** 2004. Beyond consensus: statistical free energies reveal hidden interactions in the design of a TPR motif. J. Mol. Biol. **343:**731–745.
25. **Main, E. R., Y. Xiong, M. J. Cocco, L. D'Andrea, and L. Regan.** 2003. Design of stable alpha-helical arrays from an idealized TPR motif. Structure **11:**497–508.
26. **Olzmann, J. A., L. Li, and L. S. Chin.** 2008. Aggresome formation and neurodegenerative diseases: therapeutic implications. Curr. Med. Chem. **15:**47–60.
27. **Pattingre, S., L. De Vries, C. Bauvy, I. Chantret, F. Cluzeaud, E. Ogier-Denis, A. Vandewalle, and P. Codogno.** 2003. The G-protein regulator AGS3 controls an early event during macroautophagy in human intestinal HT-29 cells. J. Biol. Chem. **278:**20995–21002.
28. **Pizzinat, N., A. Takesono, and S. M. Lanier.** 2001. Identification of a truncated form of the G-protein regulator AGS3 in heart that lacks the tetratricopeptide repeat domains. J. Biol. Chem. **276:**16601–16610.
29. **Sachdev, P., S. Menon, D. B. Kastner, J. Z. Chuang, T. Y. Yeh, C. Conde, A. Caceres, C. H. Sung, and T. P. Sakmar.** 2007. G protein beta gamma subunit interaction with the dynein light-chain component Tctex-1 regulates neurite outgrowth. EMBO J. **26:**2621–2632.
30. **Sanada, K., and L. H. Tsai.** 2005. G protein betagamma subunits and AGS3 control spindle orientation and asymmetric cell fate of cerebral cortical progenitors. Cell **122:**119–131.
31. **Sato, M., C. Ribas, J. D. Hildebrandt, and S. M. Lanier.** 1996. Characterization of a G-protein activator in the neuroblastoma-glioma cell hybrid NG108-15. J. Biol. Chem. **271:**30052–30060.
32. **Schaefer, M., A. Shevchenko, and J. A. Knoblich.** 2000. A protein complex containing Inscuteable and the Galpha-binding protein Pins orients asymmetric cell divisions in Drosophila. Curr. Biol. **10:**353–362.
33. **Sha, Y., L. Pandit, S. Zeng, and N. T. Eissa.** 2009. A critical role for CHIP in the aggresome pathway. Mol. Cell. Biol. **29:**116–128.
34. **Singhvi, A., and G. Garriga.** 2009. Asymmetric divisions, aggresomes and apoptosis. Trends Cell Biol. **19:**1–7.
35. **Spiegelberg, B. D., and H. E. Hamm.** 2005. G betagamma binds histone deacetylase 5 (HDAC5) and inhibits its transcriptional co-repression activity. J. Biol. Chem. **280:**41769–41776.
36. **Takesono, A., M. J. Cismowski, C. Ribas, M. Bernard, P. Chung, S. Hazard III, E. Duzic, and S. M. Lanier.** 1999. Receptor-independent activators of heterotrimeric G-protein signaling pathways. J. Biol. Chem. **274:**33202–33205.
37. **Thomas, C. J., G. G. Tall, A. Adhikari, and S. R. Sprang.** 2008. Ric-8A catalyzes guanine nucleotide exchange on G alphai1 bound to the GPR/GoLoco exchange inhibitor AGS3. J. Biol. Chem. **283:**23150–23160.
38. **Yao, L., K. McFarland, P. Fan, Z. Jiang, Y. Inoue, and I. Diamond.** 2005. Activator of G protein signaling 3 regulates opiate activation of protein kinase A signaling and relapse of heroin-seeking behavior. Proc. Natl. Acad. Sci. U. S. A. **102:**8746–8751.
39. **Yao, L., K. McFarland, P. Fan, Z. Jiang, T. Ueda, and I. Diamond.** 2006. Adenosine A2a blockade prevents synergy between mu-opiate and cannabinoid CB1 receptors and eliminates heroin-seeking behavior in addicted rats. Proc. Natl. Acad. Sci. U. S. A. **103:**7877–7882.
40. **Yoon, E. J., H. E. Hamm, and K. P. Currie.** 2008. G protein betagamma subunits modulate the number and nature of exocytotic fusion events in adrenal chromaffin cells independent of calcium entry. J. Neurophysiol. **100:**2929–2939.
41. **Young, A., E. B. Powelson, I. E. Whitney, M. A. Raven, S. Nusinowitz, M. Jiang, L. Birnbaumer, B. E. Reese, and D. B. Farber.** 2008. Involvement of OA1, an intracellular GPCR, and G alpha i3, its binding protein, in melanosomal biogenesis and optic pathway formation. Invest. Ophthalmol. Vis. Sci. **49:**3245–3252.
42. **Yu, F., C. T. Ong, W. Chia, and X. Yang.** 2002. Membrane targeting and asymmetric localization of Drosophila partner of Inscuteable are discrete steps controlled by distinct regions of the protein. Mol. Cell. Biol. **22:**4230–4240.